

Least-Squares Estimator for Cumulative INAR(∞) Processes

Xiao-Hong Duan^{1*}, Ying-Li Wang^{1*}, Ping He^{1**}

¹ School of Mathematics, SHUFE
isduanxh@163.com, 2022310119@163.sufe.edu.cn, pinghe@mail.shufe.edu.cn

* These authors contributed equally to this work.

** Corresponding author: Ping He (pinghe@mail.shufe.edu.cn)

Abstract

We explore the cumulative INAR(∞) process, an infinite-order extension of integer-valued autoregressive models, providing deeper insights into count time series of infinite order. Introducing a novel framework, we define a distance metric within the parameter space of the INAR(∞) model, which improves parameter estimation capabilities. Employing a least-squares estimator, we derive its theoretical properties, demonstrating its equivalence to a norm-based metric and establishing its optimality within this framework.

To validate the estimator's performance, we conduct comprehensive numerical experiments with sample sizes $T = 200$ and $T = 500$. These simulations reveal that the estimator accurately recovers the true parameters and exhibits asymptotic normality, as confirmed by statistical tests and visual assessments such as histograms and Q-Q plots. Our findings provide empirical support for the theoretical underpinnings of the cumulative INAR(∞) model and affirm the efficacy of the proposed estimation method. This work not only deepens the understanding of infinite-order count time series models but also establishes parallels with continuous-time Hawkes processes.

Keywords: Least Squares Estimator; discrete Hawkes processes; cumulative INAR(∞) processes
MSC2020: 62M10; 62F12; 60J80

1 Introduction

The INAR(∞) process is an integer-valued time series model that extends the traditional INAR(p) processes to infinite order (see, for example, Kirchner (2016)). For $\alpha_k \geq 0$, where k is a non-negative integer, let $(\epsilon_n)_{n \in \mathbb{Z}}$ be i.i.d. Poisson(α_k) random variables, and let $\xi_l^{(n,k)}$ be Poisson(α_k) random variables. These variables are mutually independent for different $n \in \mathbb{Z}$, $k \in \mathbb{N}$, and $l \in \mathbb{N}$, and they are also independent of the sequence $(\epsilon_n)_{n \in \mathbb{Z}}$.

An INAR(∞) process is a sequence of random variables $(X_n)_{n \in \mathbb{Z}}$ that satisfies the following system of stochastic difference equations:

$$\epsilon_n = X_n - \sum_{k=1}^{\infty} \alpha_k \circ X_{n-k} = X_n - \sum_{k=1}^{\infty} \sum_{l=1}^{X_{n-k}} \xi_l^{(n,k)}, \quad n \in \mathbb{Z},$$

where the operator “ \circ ”, called the **reproduction operator**, is defined as $\alpha \circ Y := \sum_{n=1}^Y \xi_n^{(\alpha)}$, for a random variable Y that takes non-negative integer values and a constant $\alpha \geq 0$. Here, $(\xi_n^{(\alpha)})_{n \in \mathbb{N}}$ are i.i.d. Poisson(α) random variables and are independent of Y . We refer to $\xi_n^{(\alpha)}$ as the **offspring variable**, and to $(\xi_n^{(\alpha)})$ as the **offspring sequence**. Additionally, we call ν the **immigration parameter**, (ϵ_n) the **immigration sequence**, and $\alpha_k \geq 0$ the **reproduction coefficient** for each non-negative integer k .

A cumulative INAR(∞) process, also known as a discrete Hawkes process, is defined by $N_n = \sum_{s=1}^n X_s$. Hawkes processes, introduced by Hawkes (1971), are continuous-time self-exciting point processes widely used in various fields. A general Hawkes process is a simple point process N admitting an $\mathcal{F}_t^{-\infty}$ intensity

$$\lambda_t := \lambda \left(\int_{-\infty}^t h(t-s) N(ds) \right),$$

where $\lambda(\cdot) : \mathbb{R}^+ \rightarrow \mathbb{R}^+$ is locally integrable and left continuous, $h(\cdot) : \mathbb{R}^+ \rightarrow \mathbb{R}^+$, and we always assume that $\|h\|_{L^1} = \int_0^{\infty} h(t) dt < \infty$. We always assume that $N(-\infty, 0] = 0$, i.e. the Hawkes process has empty history. In the literature, $h(\cdot)$ and $\lambda(\cdot)$ are usually referred to as the exciting function and the rate function, respectively. The Hawkes process is linear if $\lambda(\cdot)$ is linear and it is nonlinear otherwise, in the linear case, the stochastic intensity can be written as

$$\lambda_t = \nu + \int_0^{t-} h(t-s) N(ds).$$

Discrete-time analogs, such as cumulative INAR(∞) processes, offer similar modeling capabilities with a focus on count data observed at fixed time intervals. Under certain conditions, the Poisson autoregressive process can be viewed as an INAR(∞) process with Poisson offspring. For a com-

prehensive discussion of Poisson autoregressive models and their connections to INAR and Hawkes processes, refer to Fokianos (2021) and Huang and Khabou (2023). It is easy to see that if we let an INAR(∞) process $(X_n)_{n \geq 1}$ start from time 1 ($X_1 \sim \text{Poisson}(\nu)$), it can also be defined by:

$$\lambda_n = \nu + \sum_{s=1}^{n-1} \alpha_{n-s} X_s, \quad (1.1)$$

where $\nu > 0$ is the immigration rate, and $(\alpha_n)_{n \geq 1} \in \ell^1$ represents the offspring distribution, with $\alpha_n \geq 0$ for all $n \in \mathbb{N}$. Given the history \mathcal{F}_{n-1} , the count X_n follows a Poisson distribution with parameter λ_n , i.e.,

$$X_n \mid \mathcal{F}_{n-1} \sim \text{Poisson}(\lambda_n).$$

INAR(∞) processes are very powerful tools for estimating Hawkes processes; see for example, Kirchner (2017).

In this paper, we propose a new perspective on understanding the INAR(∞) process, which is useful for deriving a distance in the parameter space. The INAR(∞) process is in fact a series of discretized time observations of a continuous-time linear Hawkes process, where the exciting function is

$$h(t) = \sum_{k=1}^{\infty} \alpha_k \delta_{\{t=k\}}, \quad (1.2)$$

where δ is the generalized Delta function. This can be understood from the immigration-birth representation of the continuous-time Hawkes process. Consider the population of a region: if an immigrant arrives at time t (either as a descendant of a former immigrant or from another region), the number of descendants of the immigrant at time $t + n$ follows a Poisson distribution with parameter α_n . Denote X_n as the increase in population volume in the time interval $(n - 1, n]$; then it consists of two parts:

1. The first part is the number of new immigrants from other regions, which follows a Poisson distribution with parameter ν .
2. The second part is the number of descendants from before time n , which follows a Poisson distribution with parameter $\sum_{k=1}^{n-1} \alpha_k X_{n-k}$.

As a result, $X_n \mid \mathcal{F}_{n-1} \sim \text{Poisson}(\nu + \sum_{k=1}^{n-1} \alpha_k X_{n-k})$.

2 Main Results

The technical method in this paper is inspired by Reynaud-Bouret and Schbath (2010). Let us give some notations first. In this paper, $\|\cdot\|_1$ and $\|\cdot\|_2$ denote the usual ℓ^1 -norm and ℓ^2 -norm, respectively. We also set $(A_n)_{n \geq 1} \in \ell^1$ as the sequence defined on \mathbb{N} by $A_n = \sum_{k=1}^{\infty} (\alpha)_n^{*k}$, where $*$ denotes the discrete convolution which means for two non-negative sequences $(q_n)_{n \geq 1}, (m_n)_{n \geq 1} \in \ell^1$, $(q * m)(n) = \sum_{s=1}^{n-1} q_s m_{n-s}$, and $\alpha^{*(k+1)}$ denotes the discrete convolution of α^{*k} with α , i.e., $\alpha^{*(k+1)} = \alpha * \alpha^{*k}$. $(A_n)_{n \geq 1}$ is well defined since $\|\alpha\|_1 < 1$.

2.1 Problem Formulation

The parameter we aim to estimate is $s = (\nu, \alpha)$, where $\alpha = (\alpha_1, \alpha_2, \dots)$. Since observational data are always finite, we introduce a sufficiently large integer T (with T increasing as the data length increases). Then, we estimate $s = (\nu, \alpha_1, \alpha_2, \dots, \alpha_{T-1})$. We assume $\sum_{k=1}^{T-1} \alpha_k < 1$ to ensure the stationarity of the process.

The parameter space is a Euclidean space

$$\mathfrak{l}^2 = \{f : f = (\mu, \beta) = (\mu, \beta_1, \beta_2, \dots, \beta_{T-1})\}$$

equipped with the inner product $\langle \cdot, \cdot \rangle$, where for $f = (\mu, \beta)$ and $g = (\xi, \gamma)$ in \mathfrak{l}^2 , $\langle f, g \rangle = \mu\xi + \sum_{k=1}^{T-1} \beta_k \gamma_k$.

2.2 Least-Squares Contrast

For $f = (\mu, \beta) \in \mathfrak{l}^2$, we define the intensity candidates as

$$\Phi_f(n) := \mu + \sum_{k=1}^{n-1} \beta_k X_{n-k},$$

and, in particular, $\Phi_s(n) = \lambda_n$. We want to estimate the intensity $\Phi_s(n)$. The estimator $\Phi_f(n)$ should be sufficiently close to $\Phi_s(n)$. For every $f \in \mathfrak{l}^2$, we define a Least-Squares Contrast:

$$\gamma_T(f) := -\frac{2}{T} \sum_{n=1}^T \Phi_f(n) X_n + \frac{1}{T} \sum_{n=1}^T \Phi_f^2(n).$$

Now, let's prove that $\gamma_T(f)$ can be used as a metric to measure the distance between $\Phi_f(n)$ and $\Phi_s(n)$. First, for every $f \in \ell^2$, we define

$$D_T^2(f) := \frac{1}{T} \sum_{n=1}^T \Phi_f^2(n) \text{ and } \|f\|_D := \sqrt{\mathbb{E}[D_T^2(f)]}.$$

Proposition 2.4 guarantees that D_T^2 is a quadratic form and that $\|f\|_D$ is equivalent to $\|f\|_2$. To prove Proposition 2.4, we first introduce some technical lemmas.

Lemma 2.1 (Solution of Discrete Renewal Equations). *Given a non-negative sequence $(\alpha_n)_{n \geq 1} \in \ell^1$ and two non-negative sequences $(x_n)_{n \geq 1}$, $(y_n)_{n \geq 1}$, the following equation*

$$x_n = y_n + \sum_{s=1}^{n-1} \alpha_s x_{n-s} \quad (2.1)$$

has the unique solution $x_n = (y + y * A)(n) = y_n + \sum_{i=1}^{n-1} A_i y_{n-i}$.

The proof of this lemma is omitted, we refer the reader to Lemma 4.1 in Cai et al. (2024). From Lemma 2.1, we can easily obtain an upper bound for $\mathbb{E}[\lambda_n]$. In fact, taking the expectation on both sides of (1.1), we have $\mathbb{E}[X_n] = \nu + \sum_{s=1}^{n-1} \alpha_{n-s} \mathbb{E}[X_s]$. Using Lemma 2.1, it follows that

$$\mathbb{E}[\lambda_n] = \mathbb{E}[X_n] \leq \frac{\nu}{1 - \|\alpha\|_1}. \quad (2.2)$$

An upper bound of $\mathbb{E}[X_n^2]$ is obtained when $\|\alpha\|_2^2 < \frac{1}{2}$,

$$\mathbb{E}[X_n^2] - \mathbb{E}[\lambda_n] = \mathbb{E}[\lambda_n^2] = \mathbb{E} \left[\left(\nu + \sum_{k=1}^{n-1} \alpha_k X_{n-k} \right)^2 \right] \leq 2\mathbb{E} \left[\nu^2 + \sum_{k=1}^{n-1} \alpha_k^2 X_{n-k}^2 \right].$$

Therefore,

$$\mathbb{E}[X_n^2] \leq \frac{2\nu^2 + \mathbb{E}[\lambda_n]}{1 - 2\|\alpha\|_2^2} \leq \frac{2\nu^2(1 - \|\alpha\|_1) + \nu}{(1 - 2\|\alpha\|_2^2)(1 - \|\alpha\|_1)}.$$

Remark 2.2. *We believe that $\|\alpha\|_2^2 < \frac{1}{2}$ appears to be a technical requirement for deriving the upper bound. In the numerical experiments, we also set $\alpha_1 = 0.8$ and $\alpha_n = 0$ for $n \geq 2$. Our results show that the relative error falls within an acceptable range, as defined in our analysis.*

Lemma 2.3. *Let $(N_n)_{n \geq 1}$ be a cumulative INAR(∞) process with $\|\alpha\|_2^2 < \frac{1}{2}$, and $\beta = (\beta_1, \beta_2, \dots) \in \ell^1$ with $\beta_k \geq 0$ for $k \geq 1$. Then, for every $n \in \mathbb{N}$,*

$$\mathbb{E} \left[\left(\sum_{k=1}^{n-1} \beta_k X_{n-k} \right)^2 \right] \leq \frac{2\nu^2(1 - \|\alpha\|_1) + \nu}{(1 - 2\|\alpha\|_2^2)(1 - \|\alpha\|_1)} \left(\sum_{k=1}^{n-1} \beta_k \right)^2.$$

Proof. First, by the Cauchy-Schwarz inequality,

$$\left(\sum_{k=1}^{n-1} \beta_k^{\frac{1}{2}} \beta_k^{\frac{1}{2}} X_{n-k} \right)^2 \leq \left(\sum_{k=1}^{n-1} \beta_k \right) \left(\sum_{k=1}^{n-1} \beta_k X_{n-k}^2 \right) = \sum_{k=1}^{n-1} \beta_k \sum_{\tau=1}^{n-1} \beta_\tau X_{n-\tau}^2,$$

taking the expectation of both sides yields

$$\begin{aligned} \mathbb{E} \left[\left(\sum_{k=1}^{n-1} \beta_k X_{n-k} \right)^2 \right] &\leq \mathbb{E} \left[\left(\sum_{k=1}^{n-1} \beta_k \sum_{\tau=1}^{n-1} \beta_\tau X_{n-\tau}^2 \right) \right] \\ &= \sum_{k=1}^{n-1} \beta_k \sum_{\tau=1}^{n-1} \beta_{n-\tau} \mathbb{E}[X_\tau^2] \\ &\leq \frac{2\nu^2(1 - \|\alpha\|_1) + \nu}{(1 - 2\|\alpha\|_2^2)(1 - \|\alpha\|_1)} \left(\sum_{k=1}^{n-1} \beta_k \right)^2. \end{aligned}$$

□

Proposition 2.4. D_T^2 is a quadratic form on ℓ^2 . Assume $\|\alpha\|_2^2 < \frac{1}{2}$, the squared expectation of D_T^2 is $\|\cdot\|_D^2$, and it satisfies the following inequality:

$$L\|f\|_2 \leq \|f\|_D \leq K\|f\|_2, \quad (2.3)$$

where

$$L^2 = \min \left\{ \frac{1}{1 + \nu T(T-1)(1 + \|\alpha\|_1)^2}, \frac{\nu}{2T(1 - \|\alpha\|_1)(1 + \|\alpha\|_1)^2} \right\},$$

and

$$K^2 = \max \left\{ 2, \frac{T-1}{2} \left[\frac{2\nu^2}{(1 - \|\alpha\|_1)^2} + \frac{2\nu^2(1 - \|\alpha\|_1) + \nu}{(1 - 2\|\alpha\|_2^2)(1 - \|\alpha\|_1)} \right] \right\}.$$

Proof. Assume $f = (\mu, \beta)$, we will compute $\|f\|_D^2$,

$$\begin{aligned} \|f\|_D^2 &= \mathbb{E}[D_T^2(f)] = \frac{1}{T} \sum_{n=1}^T \mathbb{E} \left[\Phi_f^2(n) \right] \\ &= \frac{1}{T} \sum_{n=1}^T \mathbb{E} \left[\left(\mu + \sum_{k=1}^{n-1} \beta_k X_{n-k} \right)^2 \right] \\ &= \frac{1}{T} \sum_{n=1}^T \mathbb{E} \left[\mu^2 + 2\mu \sum_{k=1}^{n-1} \beta_k X_{n-k} + \left(\sum_{k=1}^{n-1} \beta_k X_{n-k} \right)^2 \right]. \end{aligned} \quad (2.4)$$

It is easy to verify $\forall f = (\mu, \beta), g = (\lambda, \xi) \in \ell^2$,

$$\frac{1}{2}(\|f + g\|_D^2 - \|f\|_D^2 - \|g\|_D^2) = \frac{1}{T} \mathbb{E} \left[\sum_{n=1}^T \Phi_f(n) \Phi_g(n) \right],$$

and $\|f\|_D^2 = 0$ if and only if $f = 0$. Next, let's prove $\|\cdot\|_D$ is equivalent to $\|\cdot\|_2$, i.e. (2.3). For the lower bound, we rewrite (2.4), the RHS equals

$$\frac{1}{T} \sum_{n=1}^T \left(\mu + \mathbb{E} \left[\sum_{k=1}^{n-1} \beta_k X_{n-k} \right] \right)^2 + \text{Var} \left[\sum_{k=1}^{n-1} \beta_k X_{n-k} \right]. \quad (2.5)$$

For the first part, note that $\mathbb{E}[X_n] \geq \nu$, for $\theta \in (0, 1)$,

$$\begin{aligned} & \frac{1}{T} \sum_{n=1}^T \left(\mu + \mathbb{E} \left[\sum_{k=1}^{n-1} \beta_k X_{n-k} \right] \right)^2 \\ & \geq \frac{1}{T} \sum_{n=1}^T \left(\mu + \nu \sum_{k=1}^{n-1} \beta_k \right)^2 \\ & \geq \frac{1}{T} \sum_{n=1}^T \left((1-\theta)\mu^2 + (1-\frac{1}{\theta})\nu^2 \left(\sum_{k=1}^{n-1} \beta_k \right)^2 \right) \\ & \geq (1-\theta)\mu^2 + \frac{1}{T}(1-\frac{1}{\theta})\nu^2 \sum_{n=1}^T (n-1) \sum_{k=1}^{n-1} \beta_k^2, \end{aligned}$$

where the second inequality is obviously established since $\mu, \nu, \beta_k \geq 0$.

For the second part, consider first a continuous-time Hawkes process $(\tilde{N}_t)_{t \geq 0}$ with exciting function (1.2). From Brémaud and Massoulié (2001), for any $\phi \in L^1 \cap L^2$,

$$\text{Var} \left[\int_{\mathbb{R}} \phi(u) d\tilde{N}_u \right] = \int_{\mathbb{R}} |\hat{\phi}(\omega)|^2 f_{\tilde{N}}(\omega) d\omega \quad (2.6)$$

where $\hat{\phi}$ is the Fourier transform of ϕ , $\hat{\phi}(\omega) = \int_{\mathbb{R}} e^{i\omega t} \phi(t) dt$, $f_{\tilde{N}}$ is the Bartlett spectrum density of continuous-time Hawkes process \tilde{N} . Since the Fourier transform of h is

$$\hat{h}(\omega) = \sum_{k=1}^{\infty} \alpha_k \int_{\mathbb{R}} e^{i\omega t} \delta_{\{t=k\}} dt = \sum_{k=1}^{\infty} \alpha_k e^{i\omega k},$$

$$f_{\tilde{N}}(\omega) = \frac{\nu}{2\pi(1 - \|\alpha\|_1)|1 - \hat{h}(\omega)|^2} = \frac{\nu}{2\pi(1 - \|\alpha\|_1)|1 - \sum_{k=1}^{\infty} \alpha_k e^{i\omega k}|^2}.$$

Given $n \in \mathbb{N}$, let

$$\phi(t) = \phi_n(t) := \beta_{n-[t]-1} \mathbf{1}_{\{0 < t < n\}} = \beta_{[n-t]} \mathbf{1}_{\{t < n\}} = g(n-t) \mathbf{1}_{\{t < n\}},$$

set $\beta_0 = 0$ for convenience, since g has a positive support, $\hat{\phi}(\omega) = e^{i\omega t} \hat{g}(-\omega)$. Hence,

$$\text{Var} \left[\int_{\mathbb{R}} \phi(u) d\tilde{N}_u \right] = \int_{\mathbb{R}} |\hat{g}(-\omega)|^2 f_{\tilde{N}}(\omega) d\omega.$$

Since $f_{\tilde{N}}(\omega) \geq \frac{\nu}{2\pi(1-\|\alpha\|_1)(1+\|\alpha\|_1)^2}$, and due to the Plancherel's identity, i.e.

$$\int_{\mathbb{R}} |\hat{g}(-\omega)|^2 d\omega = 2\pi \sum_{k=1}^{n-1} \beta_k^2,$$

we obtain

$$\text{Var} \left[\int_{\mathbb{R}} \phi(u) d\tilde{N}_u \right] \geq \frac{\nu}{(1-\|\alpha\|_1)(1+\|\alpha\|_1)^2} \sum_{k=1}^{n-1} \beta_k^2.$$

Hence, set $c = \frac{\nu}{2\pi(1-\|\alpha\|_1)(1+\|\alpha\|_1)^2}$,

$$\begin{aligned} \text{Var} \left[\sum_{u=1}^{n-1} \beta_{n-u} X_u \right] &= \text{Var} \left[\int_{\mathbb{R}} \beta_{n-\lfloor u \rfloor - 1} 1_{\{u < n\}} d\tilde{N}_u \right] \\ &= \text{Var} \left[\int_{\mathbb{R}} \phi(u) d\tilde{N}_u \right] \geq 2\pi c \sum_{k=1}^{n-1} \beta_k^2. \end{aligned}$$

Combine them together,

$$\begin{aligned} \|f\|_D^2 &\geq (1-\theta)\mu^2 + (1-\frac{1}{\theta})\nu^2 \frac{1}{T} \sum_{n=1}^T \left((n-1) \sum_{k=1}^{n-1} \beta_k^2 + 2\pi c \sum_{k=1}^{n-1} \beta_k^2 \right) \\ &\geq (1-\theta)\mu^2 + \left[(1-\frac{1}{\theta})\nu^2 \frac{T-1}{2} + \frac{2\pi c}{T} \right] \sum_{k=1}^{T-1} \beta_k^2. \end{aligned}$$

Choose θ satisfying $(1-\frac{1}{\theta})\nu^2 \frac{T-1}{2} + \frac{2\pi c}{T} = \frac{\pi c}{T}$, i.e.

$$\theta = \frac{\nu T(T-1)(1+\|\alpha\|_1)^2}{1+\nu T(T-1)(1+\|\alpha\|_1)^2},$$

then

$$\|f\|_D^2 \geq \frac{1}{1+\nu T(T-1)(1+\|\alpha\|_1)^2} \mu^2 + \frac{\nu}{2T(1-\|\alpha\|_1)(1+\|\alpha\|_1)^2} \sum_{k=1}^{T-1} \beta_k^2.$$

Finally we obtain

$$L^2 = \min \left\{ \frac{1}{1+\nu T(T-1)(1+\|\alpha\|_1)^2}, \frac{\nu}{2T(1-\|\alpha\|_1)(1+\|\alpha\|_1)^2} \right\}.$$

For the upper bound, from (2.5) we can see

$$\|f\|_D^2 \leq \frac{1}{T} \sum_{n=1}^T \left\{ \left(\mu + \frac{\nu}{1-\|\alpha\|_1} \sum_{k=1}^{n-1} \beta_k \right)^2 + \mathbb{E} \left[\left(\sum_{k=1}^{n-1} \beta_k X_{n-k} \right)^2 \right] \right\}.$$

For the first term inside the curly braces on the RHS, it is bounded by the following

$$\left(\mu + \frac{\nu}{1 - \|\alpha\|_1} \sum_{k=1}^{n-1} \beta_k\right)^2 \leq 2\mu^2 + 2\frac{\nu^2}{(1 - \|\alpha\|_1)^2} \left(\sum_{k=1}^{n-1} \beta_k\right)^2.$$

By Lemma 2.3,

$$\mathbb{E} \left[\left(\sum_{k=1}^{n-1} \beta_k X_{n-k}\right)^2 \right] \leq \frac{2\nu^2(1 - \|\alpha\|_1) + \nu}{(1 - 2\|\alpha\|_2^2)(1 - \|\alpha\|_1)} \left(\sum_{k=1}^{n-1} \beta_k\right)^2.$$

Hence,

$$\begin{aligned} \|f\|_D^2 &\leq 2\mu^2 + \left[\frac{2\nu^2}{(1 - \|\alpha\|_1)^2} + \frac{2\nu^2(1 - \|\alpha\|_1) + \nu}{(1 - 2\|\alpha\|_2^2)(1 - \|\alpha\|_1)} \right] \cdot \frac{1}{T} \sum_{n=1}^T \left(\sum_{k=1}^{n-1} \beta_k\right)^2 \\ &\leq 2\mu^2 + \left[\frac{2\nu^2}{(1 - \|\alpha\|_1)^2} + \frac{2\nu^2(1 - \|\alpha\|_1) + \nu}{(1 - 2\|\alpha\|_2^2)(1 - \|\alpha\|_1)} \right] \frac{1}{T} \sum_{n=1}^T (n-1) \sum_{k=1}^{n-1} \beta_k^2 \\ &\leq 2\mu^2 + \left[\frac{2\nu^2}{(1 - \|\alpha\|_1)^2} + \frac{2\nu^2(1 - \|\alpha\|_1) + \nu}{(1 - 2\|\alpha\|_2^2)(1 - \|\alpha\|_1)} \right] \left(\frac{T-1}{2}\right) \sum_{k=1}^{T-1} \beta_k^2. \end{aligned}$$

Finally we obtain,

$$K^2 = \max \left\{ 2, \frac{T-1}{2} \left[\frac{2\nu^2}{(1 - \|\alpha\|_1)^2} + \frac{2\nu^2(1 - \|\alpha\|_1) + \nu}{(1 - 2\|\alpha\|_2^2)(1 - \|\alpha\|_1)} \right] \right\}.$$

□

Then we can give our main theorem.

Theorem 2.5. *Let $(N_n)_{n \geq 1}$ be a cumulative INAR(∞) process with $\|\alpha\|_1 < 1$ and $\|\alpha\|_2^2 < \frac{1}{2}$, for any $f \in \mathcal{I}^2$, define*

$$\gamma_T(f) := -\frac{2}{T} \sum_{n=1}^T \Phi_f(n) X_n + \frac{1}{T} \sum_{n=1}^T \Phi_f^2(n),$$

then $\gamma_T(f)$ is a contrast, i.e. $\mathbb{E}[\gamma_T(f)]$ reaches its minimum when $f = s$.

Proof. By the bilinear property of $D_T^2(f)$ and the Iterated expectation theorem, we obtain

$$\begin{aligned}
\mathbb{E}[\gamma_T(f)] &= \mathbb{E}\left[-\frac{2}{T}\sum_{n=1}^T\Phi_f(n)X_n\right] + \mathbb{E}\left[\frac{1}{T}\sum_{n=1}^T\Phi_f^2(n)\right] \\
&= \mathbb{E}\left[-\frac{2}{T}\sum_{n=1}^T\Phi_f(n)\Phi_s(n)\right] + \mathbb{E}[D_T^2(f)] \\
&= \mathbb{E}\left[-\frac{2}{T}\sum_{n=1}^T\Phi_f(n)\Phi_s(n)\right] + \|f\|_D^2 \\
&= \mathbb{E}\left[\frac{1}{T}\sum_{n=1}^T(\Phi_f(n) - \Phi_s(n))^2\right] - \mathbb{E}\left[\frac{1}{T}\sum_{n=1}^T\Phi_s^2(n)\right] \\
&= \|f - s\|_D^2 - \|s\|_D^2.
\end{aligned}$$

From Proposition 2.4, $\|\cdot\|_D$ is a norm. As a result, $\mathbb{E}[\gamma_T(f)]$ reaches its minimum when $f = s$. \square

Finally, we will give the exact expression of $\gamma_T(f)$ as follows,

$$\begin{aligned}
\gamma_T(f) &= -\frac{2}{T}\sum_{n=1}^T\Phi_f(n)X_n + \frac{1}{T}\sum_{n=1}^T\Phi_f^2(n) \\
&= -\frac{2}{T}\sum_{n=1}^T\left(\mu + \sum_{k=1}^{n-1}\beta_k X_{n-k}\right)X_n + \frac{1}{T}\sum_{n=1}^T\left(\mu + \sum_{k=1}^{n-1}\beta_k X_{n-k}\right)^2 \\
&= -2\left[\left(\frac{1}{T}\sum_{n=1}^T X_n\right)\mu + \sum_{k=1}^{T-1}\left(\frac{1}{T}\sum_{n=k+1}^T X_{n-k}X_n\right)\beta_k\right] \\
&\quad + \mu^2 + \sum_{k=1}^{T-1}\beta_k^2\left(\frac{1}{T}\sum_{n=k+1}^T X_{n-k}^2\right) + 2\sum_{k=1}^{T-1}\mu\beta_k\left(\frac{1}{T}\sum_{n=k+1}^T X_{n-k}\right) \\
&\quad + 2\sum_{i=1}^{T-1}\sum_{j=i+1}^{T-1}\beta_i\beta_j\left(\frac{1}{T}\sum_{n=j+1}^T X_{n-i}X_{n-j}\right).
\end{aligned}$$

Assume $\boldsymbol{\theta}$ to be the T -dimensional vector consisting of the parameters to be estimated,

$$\boldsymbol{\theta} = (\mu, \beta_1, \dots, \beta_k, \dots, \beta_{T-1})^\top.$$

then we can rewrite $\gamma_T(f)$ into the following form:

$$\gamma_T(f) = -2\boldsymbol{\theta}^\top \mathbf{b} + \boldsymbol{\theta}^\top \mathbf{Y} \boldsymbol{\theta},$$

where

$$\mathbf{b} = \left(\frac{1}{T}N_T, \frac{1}{T}\sum_{n=2}^T X_{n-1}X_n, \dots, \frac{1}{T}\sum_{n=k+1}^T X_{n-k}X_n, \dots, \frac{1}{T}\sum_{n=T}^T X_1X_n\right)^\top,$$

and

$$\mathbf{Y} = \begin{pmatrix} 1 & \frac{1}{T} \sum_{n=2}^T X_{n-1} & \cdots & \frac{1}{T} \sum_{n=k+1}^T X_{n-k} & \cdots & \frac{1}{T} X_1 \\ \frac{1}{T} \sum_{n=2}^T X_{n-1} & \frac{1}{T} \sum_{n=2}^T X_{n-1}^2 & \cdots & \frac{1}{T} \sum_{n=k+1}^T X_{n-k} X_{n-1} & \cdots & \frac{1}{T} X_1 X_{T-1} \\ \frac{1}{T} \sum_{n=3}^T X_{n-2} & \frac{1}{T} \sum_{n=3}^T X_{n-1} X_{n-2} & \cdots & \frac{1}{T} \sum_{n=k+1}^T X_{n-k} X_{n-2} & \cdots & \frac{1}{T} X_1 X_{T-2} \\ \vdots & \vdots & \ddots & \vdots & \vdots & \vdots \\ \frac{1}{T} \sum_{n=k+1}^T X_{n-k} & \frac{1}{T} \sum_{n=k+1}^T X_{n-1} X_{n-k} & \cdots & \frac{1}{T} \sum_{n=k+1}^T X_{n-k}^2 & \cdots & \frac{1}{T} X_1 X_{T-k} \\ \frac{1}{T} \sum_{n=k+2}^T X_{n-k-1} & \frac{1}{T} \sum_{n=k+2}^T X_{n-1} X_{n-k-1} & \cdots & \frac{1}{T} \sum_{n=k+2}^T X_{n-k} X_{n-k-1} & \cdots & \frac{1}{T} X_1 X_{T-k-1} \\ \vdots & \vdots & \vdots & \vdots & \ddots & \vdots \\ \frac{1}{T} X_1 & \frac{1}{T} X_{T-1} X_1 & \cdots & \frac{1}{T} X_{T-k} X_1 & \cdots & \frac{1}{T} X_1^2 \end{pmatrix},$$

precisely,

$$\mathbf{Y} = (Y_{ij}) = \begin{cases} 1, & i = j = 1, \\ \frac{1}{T} \sum_{n=\max\{i,j\}}^T X_{n-\max\{i,j\}+1}, & i \neq j, i \text{ or } j = 1, \\ \frac{1}{T} \sum_{n=\max\{i,j\}}^T X_{n-i+1} X_{n-j+1}, & \text{otherwise.} \end{cases}$$

By using the conclusion of the general least squares method, the $\hat{\boldsymbol{\theta}}$ that minimizes $\gamma_T(f)$ satisfies $\mathbf{Y}\hat{\boldsymbol{\theta}} = \mathbf{b}$. If \mathbf{Y} has an inverse, we obtain the best estimator

$$\hat{\boldsymbol{\theta}} = \mathbf{Y}^{-1}\mathbf{b}.$$

It is crucial to recognize that the notion of “best” is inherently tied to the norm $\|\cdot\|_D$ as defined initially. Proposition 2.4 establish that $\|\cdot\|_D$ is indeed a norm. Furthermore, Theorem 2.5 establish that $\mathbb{E}[\gamma_T(f)]$ can be expressed as $\|f - s\|_D^2 - \|s\|_D^2$. Within this framework, $\gamma_T(f)$ serves as an empirical representation of $\|f - s\|_D^2 - \|s\|_D^2$, aligning with the conventional approach in Least-Squares Contrasts. Consequently, the estimator $\hat{\boldsymbol{\theta}}$ is optimized to minimize $\gamma_T(f)$ under the norm $\|\cdot\|_D$, thereby qualifying as the “best” estimator. We will further substantiate the practical efficacy of this estimation technique through numerical experiments.

3 Numerical Experiments(Consistency of the estimator)

In this section, we illustrate the performance of the proposed least-squares estimator for the cumulative INAR(∞) [c-INAR(∞)] model via numerical experiments. First, we describe how to generate a single realization of a INAR($T - 1$) process (Algorithm 1). Then, in Algorithm 2, we show how to repeat the simulation multiple times, form an average sequence, and compute the least-squares estimator (LSE). Finally, we present and discuss the estimation accuracy.

3.1 Simulation of a Single Realization

We begin by simulating one path of length T from a c-INAR($T - 1$) process. Let $\nu > 0$ be the immigration rate, and let $\alpha_{\text{func}}(\cdot)$ be the offspring function such that

$$X_n \mid \mathcal{F}_{n-1} \sim \text{Poisson}\left(\nu + \sum_{k=1}^{n-1} \alpha_{\text{func}}(n-k) X_k\right).$$

Algorithm 1 outlines this procedure in detail.

Algorithm 1 Part A: Simulating a single c-INAR(∞) realization

Require: Sample size T ; true immigration rate ν ; offspring function $\alpha_{\text{func}}(\cdot)$.

- 1: Initialize an array X of length T to store the realization.
 - 2: Draw $X_1 \sim \text{Poisson}(\nu)$.
 - 3: **for** $n = 2$ **to** T **do**
 - 4: Compute $\lambda_n \leftarrow \nu + \sum_{k=1}^{n-1} \alpha_{\text{func}}(n-k) \cdot X_k$.
 - 5: Sample $X_n \sim \text{Poisson}(\lambda_n)$.
 - 6: **end for**
 - 7: **Output:** The sequence $(X_n)_{1 \leq n \leq T}$.
-

3.2 Multiple Replications and Least-Squares Estimation

To estimate the parameter vector (including $\hat{\nu}$ and $\hat{\alpha}_1, \dots, \hat{\alpha}_{T-1}$ in finite practice), we repeat the simulation multiple times, accumulate an average sequence \bar{X} , and then solve a linear system derived from the least-squares contrast. Algorithm 2 summarizes the entire process for computing the LSE.

3.3 Experimental Setup and Results

We now present two numerical experiments, both experiments have number of replications $N_{\text{experiments}} = 1000$. Table 1 presents the estimated parameters (first five components) from two typical experiments with different true parameter settings:

Case 1: $\nu = 100$, $\alpha_n = (1/4)^n$ for $n \geq 1$.

Case 2: $\nu = 100$, $\alpha_1 = 0.8$, and $\alpha_n = 0$ for $n \geq 2$.

Case 1 satisfies the conditions $\|\alpha\|_1 < 1$ and $\|\alpha\|_2^2 < 1/2$. In contrast, Case 2 is designed to explore whether the estimator performs well when $\|\alpha\|_2^2 > 1/2$, a scenario where our assumption may not

Algorithm 2 Part B: Accumulating results and computing the least-squares estimator

Require: Number of replications $N_{\text{experiments}}$; each replication yields $(X_n^{(i)})_{1 \leq n \leq T}$; same $T, \nu, \alpha_{\text{func}}$ as in Algorithm 1.

1: Initialize $\mathbf{X_accumulator} \leftarrow \mathbf{0}$ (length T).

2: **for** $i = 1$ **to** $N_{\text{experiments}}$ **do**

3: Run Algorithm 1 to obtain a single path $(X_1^{(i)}, \dots, X_T^{(i)})$.

4: Accumulate:

$$\mathbf{X_accumulator} \leftarrow \mathbf{X_accumulator} + (X_1^{(i)}, \dots, X_T^{(i)}).$$

5: **end for**

6: Compute the average sequence:

$$\bar{X} \leftarrow \frac{\mathbf{X_accumulator}}{N_{\text{experiments}}}.$$

7: Construct vector \mathbf{b} and matrix \mathbf{Y} from \bar{X} :

- $b_1 = \frac{1}{T} \sum_{n=1}^T \bar{X}_n$, $b_k = \frac{1}{T} \sum_{n=k}^T \bar{X}_{n-k} \bar{X}_n$, $k = 2, \dots, T$.
- $Y_{1,1} = 1$, $Y_{1,k} = Y_{k,1} = \frac{1}{T} \sum_{n=k}^T \bar{X}_{n-k}, \dots$
- $Y_{k_1, k_2} = \frac{1}{T} \sum_{n=\max\{k_1, k_2\}}^T \bar{X}_{n-k_1} \bar{X}_{n-k_2}$, $k_1, k_2 \geq 1$.

8: Solve the linear system:

$$\mathbf{Y} \hat{\boldsymbol{\theta}} = \mathbf{b}, \text{ hence } \hat{\boldsymbol{\theta}} = \mathbf{Y}^{-1} \mathbf{b}.$$

9: **Output:** Estimated parameter vector $\hat{\boldsymbol{\theta}}$ (e.g. $\hat{\nu}, \hat{\alpha}_1, \dots, \hat{\alpha}_{T-1}$).

hold.

All replications start with different random seeds. For each replication i , we generate a c-INAR($T-1$) path $(X_n^{(i)})_{1 \leq n \leq T}$ following Algorithm 1, then sum up these paths to form an “accumulator”, and finally compute the average sequence \bar{X} . Based on the least-squares contrast in Section 5 (of the main text), we construct \mathbf{b}, \mathbf{Y} from \bar{X} and solve for $\hat{\boldsymbol{\theta}}$.

Example Estimation Output The LSE accurately recovers both the immigration rate ν and the offspring coefficients $\alpha_1, \alpha_2, \dots$, demonstrating acceptable accuracy. Additionally, the table includes the ℓ^2 -error and relative error metrics for each case to assess estimation performance quantitatively.

Table 1: Estimated Parameters and Error Metrics for Two Different True Parameter Settings

Parameter	Case 1: $\nu = 100, \alpha_n = (1/4)^n$	Case 2: $\nu = 100, \alpha_1 = 0.8, \alpha_n = 0$ for $n \geq 2$
ν	99.96	99.96
α_1	0.2499	0.8010
α_2	0.0556	-0.0084
α_3	0.0218	0.0058
α_4	0.0016	-0.0032
ℓ^2 -error ($\boldsymbol{\theta}$)	0.10898%	0.21585%
ℓ^2 -error ($\boldsymbol{\alpha}$)	38.44%	26.39%

For Case 1 in Table 1, the ℓ^2 -error is approximately 0.10898%, and the relative ℓ^2 -error for the offspring coefficients is 38.44%. This indicates a high level of accuracy in estimating the immigration rate ν and a moderate accuracy in estimating the offspring coefficients $\alpha_1, \alpha_2, \dots$.

In Case 2, the ℓ^2 -error increases to approximately 0.21585%, while the relative ℓ^2 -error for the offspring coefficients decreases to 26.39%. This suggests that the estimator maintains good accuracy for the immigration rate ν but exhibits improved performance in estimating the offspring coefficients compared to Case 1. Notably, negative values in the offspring coefficients are adjusted to 0, which reduces the error. This adjustment is also applicable to Case 1.

Remark 3.1. *The consolidated table effectively demonstrates the LSE’s capability to accurately estimate both the immigration rate and offspring coefficients under different parameter settings. The inclusion of ℓ^2 -error and relative error metrics provides a quantitative measure of estimation performance, highlighting the estimator’s robustness and reliability.*

Remark 3.2. *These experiments confirm that the least-squares estimator (LSE) derived in Section 5 performs well when the sample size T is reasonably large and when the offspring coefficients (α_k) are under certain conditions. Extending this approach to alternative offspring functions or further tuning the sample size can yield a variety of insights into real-world count data models based on c -INAR(∞) processes.*

4 Numerical Experiment: Clarifying the Asymptotic Normality of the Estimator by Fixing $T = 200$ and $T = 500$

In the traditional sense, *asymptotic normality* refers to a series of estimators converging in distribution to a normal distribution as the sample size approaches infinity. However, in the context of

a cumulative INAR(∞) model, defining an infinite-dimensional normal random variable becomes challenging because the dimension of the estimator vector $\hat{\boldsymbol{\theta}}$ increases with the sample size T . As of now, we lack a comprehensive mathematical characterization of this *asymptotic normality* phenomenon for infinite-dimensional cases.

Instead, we numerically verify the asymptotic normality of the first several components of $\hat{\boldsymbol{\theta}}$ by conducting simulations at fixed sample sizes $T = 200$ and $T = 500$. The goal is to assess whether these finite-sample estimators behave “close enough” to their large-sample counterparts, thereby providing empirical support for the normal approximation in practical scenarios. We provide a *numerical* illustration by fixing the sample size at $T = 200$ and examining whether the LSE behaves “approximately normal”. Specifically, we:

1. Simulate multiple independent paths $(X_n)_{1 \leq n \leq T}$ from a c-INAR($T - 1$) model with known parameters;
2. Compute the corresponding least-squares estimator $\hat{\boldsymbol{\theta}}$ for each path;
3. Collect the estimates $(\hat{\boldsymbol{\theta}}^{(i)})$ across repeated experiments and visualize their empirical distribution via histograms and Q–Q plots;
4. Apply statistical normality tests (e.g. Jarque–Bera, Shapiro–Wilk) to see if we can reject a normal distribution hypothesis.

Algorithm 3 Numerical Verification of LSE Normality at a Fixed Sample Size $T = 200$

Require: (1) A sample length $T = 200$; (2) A true immigration rate ν ; (3) A sequence (α_k) or a function `alpha_func(k)` for $k \geq 1$.

- 1: **Initialize** number of experiments N_{rep} (e.g. $N_{\text{rep}} = 1000$).
 - 2: **for** $i \leftarrow 1$ to N_{rep} **do**
 - 3: **Simulate a single path** $(X_n)_{1 \leq n \leq T}$:
 - 4: $X_1 \leftarrow \text{Poisson}(\nu)$
 - 5: **for** $n \leftarrow 2$ to T **do**
 - 6: $\lambda_n \leftarrow \nu + \sum_{k=1}^{n-1} \alpha_k X_{n-k}$
 - 7: $X_n \leftarrow \text{Poisson}(\lambda_n)$
 - 8: **end for**
 - 9: **Compute the LSE, $\hat{\theta}^{(i)}$** , by:
 - 10: 1) *Truncating* at some order $p < T$;
 - 11: 2) Forming the vector \mathbf{b} and matrix \mathbf{Y} ;
 - 12: 3) Solving $\mathbf{Y} \hat{\theta}^{(i)} = \mathbf{b}$ if \mathbf{Y} is invertible.
 - 13: **Store** the result $\hat{\theta}^{(i)}$.
 - 14: **end for**
 - 15: **Analyze the distribution** of $(\hat{\theta}^{(i)})_{1 \leq i \leq N_{\text{rep}}}$:
 - 16: - Construct histograms for each parameter component (e.g. $\hat{\nu}$, $\hat{\alpha}_1$, ...).
 - 17: - Plot Q–Q diagrams against a normal distribution.
 - 18: - Apply normality tests (`scipy.stats.shapiro`, `jarque_bera`, etc.) to check p -values.
- Ensure:** An empirical assessment of whether $\hat{\theta}$ approximates a normal distribution for $T = 200$.
-

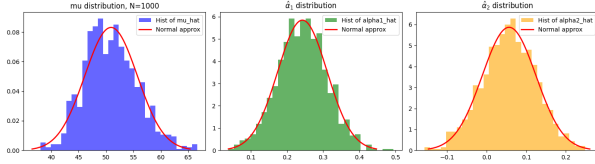
4.1 Illustrative Figures and Observations

We conducted two separate numerical experiments to assess the distribution of the least-squares estimator (LSE) at sample sizes $T = 200$ and $T = 500$. Figure 1 displays the histograms and Q–Q plots for both sample sizes, while Table 2 summarizes the Jarque–Bera and Shapiro–Wilk test p -values along with the sample means and standard deviations.

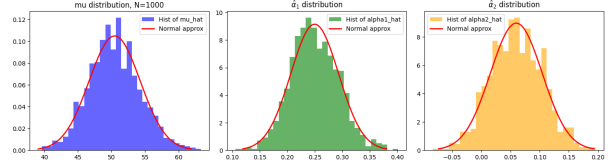
Table 2: Jarque–Bera and Shapiro–Wilk Test p -values for LSE Components at $T = 200$ and $T = 500$

Parameter	$T = 200$		$T = 500$	
	JB p-value	SW p-value	JB p-value	SW p-value
$\hat{\mu}$	0.0002	0.1106	0.1174	0.4589
$\hat{\alpha}_1$	0.7372	0.6985	0.0872	0.2456
$\hat{\alpha}_2$	0.3988	0.6192	0.5363	0.4089

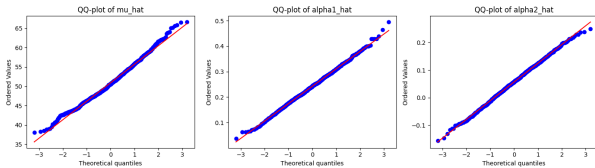
Here are results for $T = 200$ and $T = 500$.



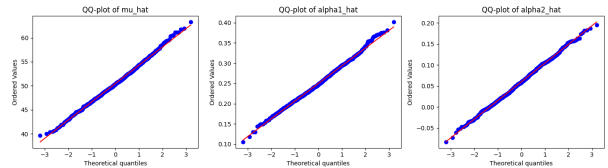
(a) Histograms of the LSE components $(\hat{\mu}, \hat{\alpha}_1, \hat{\alpha}_2)$ at $T = 200$, overlaid with normal PDF curves using the empirical means and standard deviations.



(b) Histograms of the LSE components $(\hat{\mu}, \hat{\alpha}_1, \hat{\alpha}_2)$ at $T = 500$, overlaid with normal PDF curves using the empirical means and standard deviations.



(c) Q–Q plots comparing the LSE components to a standard normal distribution at $T = 200$. Points closer to the diagonal suggest better normal approximation.



(d) Q–Q plots comparing the LSE components to a standard normal distribution at $T = 500$. Points closer to the diagonal suggest better normal approximation.

Figure 1: Histograms and Q–Q plots of the least-squares estimator (LSE) components for sample sizes $T = 200$ and $T = 500$.

Jarque–Bera Test: The p-values for the Jarque–Bera (JB) test at $T = 200$ and $T = 500$ are presented in Table 2. For $T = 200$, $\hat{\nu}$ yields a very small p-value (0.0002), suggesting a potential departure from normality and leading to the rejection of the null hypothesis at the 5% significance level. In contrast, $\hat{\alpha}_1$ and $\hat{\alpha}_2$ have p-values (0.7372 and 0.3988, respectively) that do not warrant rejection of normality. For $T = 500$, all JB p-values exceed 0.05, indicating no significant deviation from normality for any of the estimators.

Shapiro–Wilk Test: Similarly, the Shapiro–Wilk (SW) test p-values for both sample sizes are reported in Table 2. At $T = 200$, $\hat{\nu}$ has a p-value of 0.1106, which does not reject the null hypothesis of normality, despite the JB test’s indication. The other parameters also show p-values well above 0.05. At $T = 500$, all SW p-values are comfortably above 0.05, reinforcing the absence of significant departures from normality.

Sample Means and Standard Deviations: The empirical means and standard deviations for the estimators are also summarized in Table 2. For both sample sizes, the means are close to the true parameter values ($\nu = 50$, $\alpha_1 = 0.25$, $\alpha_2 = 0.0625$), with slightly reduced variability observed as T increases from 200 to 500.

Visual Assessments: Figure 1 illustrates that the histograms for $T = 500$ appear more concentrated around the fitted normal curves compared to $T = 200$. Additionally, the Q–Q plots for $T = 500$ show better alignment with the diagonal line, indicating improved normal approximation

with larger sample sizes.

Remark 4.1. Overall, for $T = 200$, $\hat{\nu}$ shows a mild discrepancy between the two tests (JB and SW), indicating potential non-normal tails. However, $\hat{\alpha}_1$ and $\hat{\alpha}_2$ appear reasonably normal at that sample size. By increasing the sample size to $T = 500$, the normal approximation becomes more robust for all three parameters, in line with the usual asymptotic intuition.

References

- Brémaud, P. and Massoulié, L. (2001). Hawkes branching point processes without ancestors. *J. Appl. Probab.*, 38(1):122–135.
- Cai, C., He, P., Wang, Q., and Wang, Y. (2024). Scaling limit of heavy-tailed nearly unstable INAR (∞) processes and rough fractional diffusions. *arXiv preprint arXiv:2403.11773*.
- Fokianos, K. (2021). Multivariate count time series modelling. *Econ. Stat.*
- Hawkes, A. (1971). Spectra of some self-exciting and mutually exciting point processes. *Biometrika*, 58(1):83–90.
- Huang, L. and Khabou, M. (2023). Nonlinear poisson autoregression and nonlinear Hawkes processes. *Stoch. Process. Appl.*, 161:201–241.
- Kirchner, M. (2016). Hawkes and INAR (∞) processes. *Stoch. Process. Appl.*, 126(8):2494–2525.
- Kirchner, M. (2017). An estimation procedure for the Hawkes process. *Quant. Finance*, 17(4):571–595.
- Reynaud-Bouret, P. and Schbath, S. (2010). Adaptive estimation for Hawkes processes; application to genome analysis. *Ann. Stat.*